An Ultrastructural Pachytene Karyotype for *Melampsora lini*

E. W. A. Boehm and W. R. Bushnell

First author: former research assistant, Department of Plant Pathology, University of Minnesota; second author: research plant physiologist, USDA-Agricultural Research Service, Cereal Rust Laboratory, University of Minnesota, St. Paul 55108.

Present address of E. W. A. Boehm: Department of Plant Pathology, University of Florida, 1453 Fifield Hall, Gainesville 32611-0513. Send reprint requests to E. W. A. Boehm.

Cooperative investigation of the Agricultural Research Service, U.S. Department of Agriculture and the Department of Plant Pathology, University of Minnesota.

We thank G. J. Lawrence (CSIRO, Division of Plant Industry, Canberra, Australia) for his insightful correspondence throughout the course of this study and G. D. Statler (Department of Plant Pathology, North Dakota State University, Fargo) for providing the isolates used in this study. We also gratefully acknowledge Rod Kuehn (Electron Microscope Laboratory, College of Biological Sciences, University of Minnesota), Gib Ahlstrand (Electron Microscope Laboratory, Department of Plant Pathology, University of Minnesota), and the staff of the Agricultural Research Service-Cereal Rust Laboratory.

Published as paper 19,698 of the Scientific Journal Series of the Minnesota Agricultural Experiment Station. Mention of a trademark name or proprietary product does not constitute a guarantee or warranty by the U.S. Department of Agriculture or the University of Minnesota and does not imply approval to the exclusion of other products that may also be suitable.

Accepted for publication 29 June 1992.

ABSTRACT

Boehm, E. W. A., and Bushnell, W. R. 1992. An ultrastructural pachytene karyotype for *Melampsora lini*. Phytopathology 82:1212-1218.

An ultrastructural karyotype was derived from five serially sectioned pachytene nuclei of two isolates of *Melampsora lini*. Each of the five reconstructed nuclei contained 18 distinct bivalents, which terminated at both ends on the nuclear envelope and represented 36 chromosomes homologously paired as synaptonemal complexes. The 18 bivalents formed a finely graded series of lengths ranging from 3.2 to 9.0% of the total length of all bivalents. No centromeres were resolved, precluding the use of the centromeric index as an aid in classification of bivalents. The only bivalent that could be identified among the five reconstructed nuclei was the one in terminal association with the nucleolus. Because no morphological changes accompany the progression of meiotic prophase I stages in the rust teliospore, nuclei at or near mid-pachynema were identified by using epifluorescence microscopy of fixed teliospore protoplasts stained with 4,6-diamidino-2-phenylindole (DAPI) from which walls were mechanically removed. The *M. lini* karyotype of $n = 18$ is significantly larger than that previously reported in the literature and agrees with the high number of virulence genes reported to segregate independently.

Additional keywords: flax rust, fungi, gene-for-gene, uredinales.

Melampsora lini (Ehrenb.) Desmaz., causal agent of flax rust on *Linum usitatissimum* L., has served as a model for understanding the genetics governing race-specific host pathogen interactions. Early studies by Flor (15–18) showed that virulence in *M. lini* to flax varieties with single genes for resistance segregated in monofactorial ratios and that virulence to varieties with two, three, and four resistance genes segregated in bi-, tri-, and tetrafactorial ratios. From these results, Flor (19) developed the gene-for-gene model that has subsequently been confirmed and extended by others to include not only flax rust (33,51), but many other host-parasite systems (reviewed by Flor [20] and Person [40]).

Single gene segregation ratios in *M. lini* have been obtained for virulence on flax differentials possessing 27 of the 30 presently known resistance genes (32,53). Some of these 27 genetic markers occur in groups in which the avirulence genes within each group are sufficiently tightly linked so that they are usually inherited as a unit. Four such groups containing four, three, three, and two avirulence genes have been identified (32). Each of these groups can represent a single locus in broad scale gene-mapping studies. As a consequence, the number of "effective" virulence loci identified in *M. lini* is not 27 but 19. Kapooria (30) estimated the haploid chromosome number of *M. lini* as $n = 5$ or 6 on the basis of light microscope observations of aceto-carmine-stained basidiospores. If the 19 loci were restricted to five or six chromosomes, then it might be expected that a greater degree of linkage would have been detected among them, even allowing that loose linkages might not be detected because of the relatively small number of progeny in most of the crosses and that some pairwise combinations of loci cannot be tested for linkage because segregation at these loci has not occurred in the same family (G. J. Lawrence, *personal communication*). The apparent disparity between the number of linkage groups identified and the estimated number of chromosomes could be due to a high frequency of crossovers at meiosis. Alternatively, the true number of chromosomes possessed by *M. lini* might be greater than the five or six estimated by Kapooria (30).

In fungi that undergo meiosis, the preferred stage for determining the karyotype is pachynema of meiotic prophase I (10,35,43,45,55). In this stage, chromosomes are present as paired homologues (i.e., bivalents) and achieve their greatest lateral condensation and cytological length in association with morphologically distinct synaptonemal complexes, as reviewed by von Wettstein et al (54). However, fungal pachytene bivalents are generally small and difficult to distinguish clearly by light microscopy, except in fungi with relatively low numbers of chromosomes (24,34,48) or in those fungi in which successful two-dimensional spreads of silver-stained pachytene bivalents allow for an accurate count (42,44).

Reliable ultrastructural analysis of fungal chromosome numbers has utilized either the two-dimensional spread technique (13,22,42) or three-dimensional reconstructions of serially sectioned pachytene nuclei (4,6–9,11,12,21,26,29,50,52,55). Fungal karyotypes derived by these methods are considered definitive because synaptonemal complex reconstructions account for all chromosomes (10,35,54). On the other hand, many fungal karyotypes derived by light microscopy have proved erroneous when re-analyzed by the pachytene reconstruction method (7,12,26, 35,52). In this paper, we present the ultrastructural pachytene

karyotype for five nuclei of two closely related North American *M. lini* isolates.

MATERIALS AND METHODS

Isolates. One isolate each of races 01 and 210 of *M. lini* were used in this study. Both were of North American origin (17) and were supplied by G. D. Statler (North Dakota State University, Fargo, ND). Races 210 and 01 are avirulent on 23 and 25 of the 29 standard flax differentials, respectively; both races are virulent on the same four differentials possessing M_1, L_9, L_1, and M_2 resistance genes. Race 210 is differentiated from 01 only on the basis of its virulence to resistance genes P (cv. Koto; CI 842) and L_{10} (cv. Bolley Golden Sel; CI 1183) (17; G. D. Statler, *personal communication*).

Telia production. Flax seedlings, cv. Bison (CI 389), were grown generally by following methods of Gold and Statler (23). Nine-day-old plants were inoculated with urediniospores of each race suspended in 3 M Fluoroinert (FC-43). After inoculation, seedlings were maintained in a dew chamber without light for 18 h and then transferred to growth chambers at 18 C with a 10-h daily light cycle.

Telia of both races developed 5–6 wk after inoculation, primarily on stems. Stem segments, 5 mm in length, bearing young telia, and characterized by yellow-orange centers with few pigmented teliospores, were harvested and immersed in the primary fixative (2% glutaraldehyde, 5% acrolein [Kodak 113-6298], 0.01% Triton X-100 in 0.1 M phosphate buffer, pH 8.0) at 4 C. Acrolein and detergent were added to increase efficiency of penetration, because teliospores of *M. lini* develop subepidermally.

Pachytene nuclear selection for ultrastructural analysis. No morphological changes accompany the progression of meiotic prophase I stages in the rust fungi. Pachynema and, indeed, all of meiotic prophase I up to diakinesis occur in a thick-walled, pigmented teliospore (7,37,38). A procedure for selecting fusion nuclei at or near mid-pachynema by epifluorescence microscopy before serial sectioning has been described previously (7). In this procedure, fixed teliospore protoplasts are stained with DAPI (4,6-diamidino-2-phenylindole) and viewed by epifluorescence microscopy. Nuclei at or near pachynema are then identified on the basis of the degree of chromatin condensation. The procedure combines the approaches of Olson and Eden (39) for generating intact, fixed meiosporangial protoplasts and those of Dresser and Giroux (13) and Raju (43) for identifying, with epifluorescence

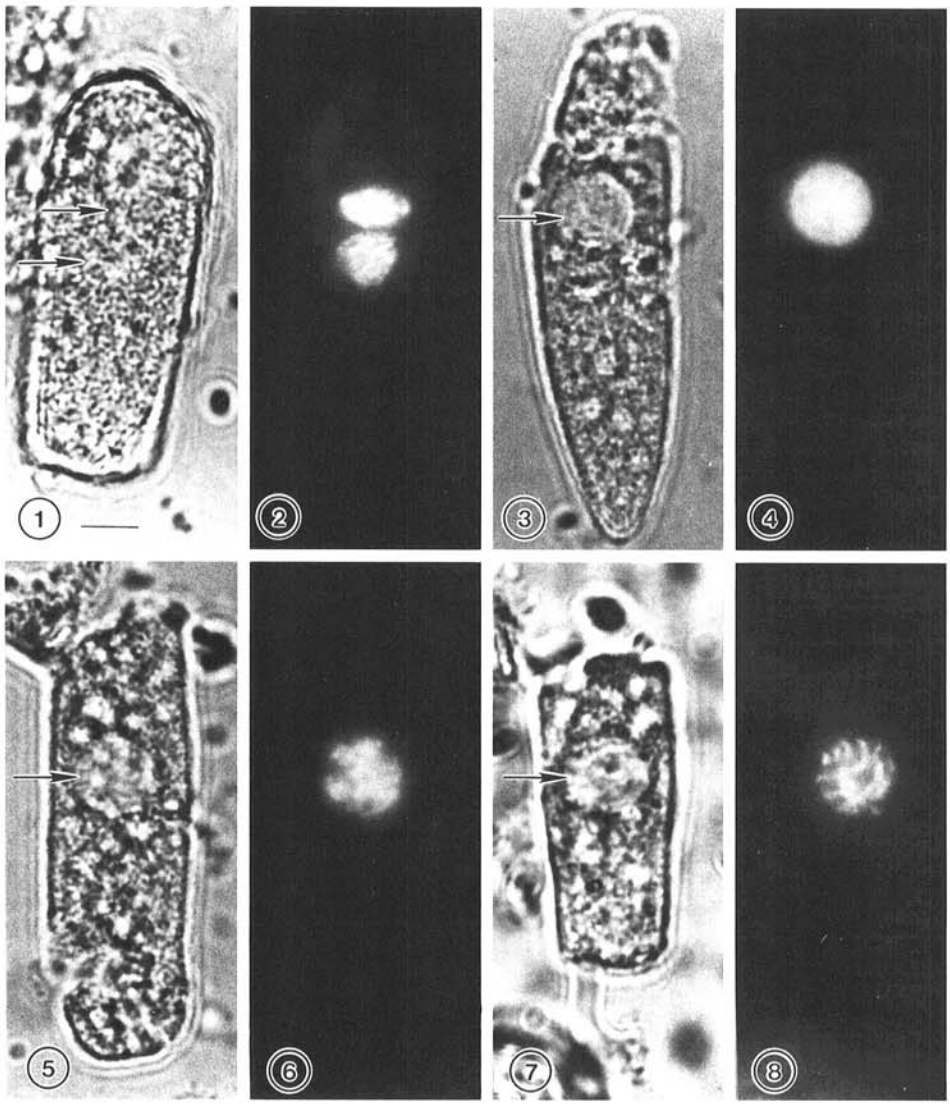

Figs. 1–8. Bright field and epifluorescence micrographs of fixed, mechanically released, DAPI-stained teliospore protoplasts of *Melampsora lini*. Each pair of figures illustrates the same protoplast viewed with either bright field (1, 3, 5, and 7) or epifluorescence microscopy (2, 4, 6, and 8). Bar = 5 μm. Arrows denote nuclei. **1** and **2,** A teliospore protoplast with two medially situated haploid, prekaryogamic nuclei. **3** and **4,** A teliospore protoplast containing a single postkaryogamic fusion nucleus that fluoresces homogeneously with little evidence of discrete chromatin. This nucleus is interpreted as being in leptonema; it has just undergone karyogamy. **5** and **6,** A teliospore protoplast containing a fusion nucleus with some degree of chromatin condensation, as compared to Figure 6, interpreted as either zygonema or diplonema. **7** and **8,** A teliospore protoplast containing a fusion nucleus with a high degree of chromatin condensation, which was interpreted as pachynema.

microscopy and DNA-binding fluorochromes, various stages of fungal meiotic prophase I, including pachynema.

Procedures for selecting nuclei, including transmission electron microscopy (TEM), three-dimensional reconstructions of serially sectioned pachytene nuclei, and derivation of karyotype and calculated bivalent lengths, were essentially as described by Boehm and McLaughlin (6). Of a total of 95 presumptive pachytene nuclei selected with epifluorescence microscopy, 32 were sectioned, and about 24 were successfully harvested as complete serial ribbons and observed ultrastructurally. Of these, 11 were photographed as a series, and five resulted in complete reconstructions. Three of the reconstructed nuclei were of race 210, and two were of race 01.

RESULTS

Teliospore protoplasts and nuclear selection. Nuclei of DAPI-stained pigmented teliospores of *M. lini* were not amenable to epifluorescence microscopy unless the wall was first removed, a situation similar to that found for *Puccinia graminis* f. sp. *tritici* (7). Although very young hyaline teliospores, harboring prekaryogamic nuclei, fluoresced without wall removal (not illustrated), any degree of wall pigmentation interfered. Mechanically releasing protoplasts from fixed teliospores allowed the degree of chromatin condensation to be directly visualized by epifluorescence microscopy so that nuclei at or near pachynema could be selected for serial sectioning and TEM.

Telia selected for this study were collected at the beginning of the sixth week after inoculation, when the majority of the teliospores were in the early stages of the pigmentation process. Protoplasts from these young telia contained both pre- and postkaryogamic nuclei, the latter in various phases of meiotic prophase I. Prekaryogamic nuclei (Figs. 1,2) were usually medially situated in the teliospore protoplast and composed about 12% of the fluorescing nuclei from these telia.

Most of the teliospores in these telia contained postkaryogamic, fusion nuclei (Figs. 3–8). More than 85% of the fusion nuclei fluoresced homogeneously and showed little, if any, evidence of discrete chromosomes (Figs. 3,4). These nuclei were presumed to have just undergone karyogamy and, thus, were in the earliest stages of meiotic prophase I (leptonema). In fungi, leptonema is characterized by relatively diffuse chromatin with a pronounced lack of lateral chromatin condensation (13,48,54,55).

As meiotic prophase I proceeds, successive degrees of chromatin condensation occur as the homologous pairs of chromosomes prepare for synapsis (zygonema), culminating in the highest degree of lateral chromatin condensation in pachynema, followed by decondensation in diplonema and diakinesis (54,55). Figures 5–8 illustrate two of these latter meiotic prophase I stages. The fusion nucleus in Figure 6 is interpreted as being either in zygonema or in diplonema (i.e., characterized by a degree of chromatin condensation intermediate between pachynema and either leptonema or diakinesis). Assignment of this nucleus to either zygonema or diplonema was not possible because these stages are not readily identified with epifluorescence microscopy (13). Non-pachytene nuclei (Fig. 6) often contained degrees of chromatin condensation similar to those found in pachytene nuclei (Fig. 8) and were sometimes selected by mistake.

Pachytene nuclei selected for serial sectioning in this study resembled the one illustrated in Figure 8. Typically, these nuclei possessed highly condensed fluorescing strands. The strands could not be seen clearly enough to derive the chromosome number but were interpreted as bivalents indicative of pachynema. These nuclear types composed about 4% of the fluorescing fusion nucleus population. Pachynema was verified in such nuclei by the presence of distinct synaptonemal complexes at the ultrastructural level when the same cell viewed with epifluorescence microscopy was serially sectioned for TEM.

Reconstructions of synaptonemal complexes. An entire *M. lini* pachytene nucleus (nucleus A, Table 1), serially sectioned to display the continuity of synaptonemal complex profiles from section to section, is presented in Figures 9–38. Full reconstructions of this nucleus are presented in Figures 39 and 40. This series of micrographs illustrates the process by which fragments of the tripartite synaptonemal complex, in consecutive sections, may be followed to determine the individuality of each bivalent and the karyotype. Bivalents are dispersed, as if by repulsion, so that the distance from each to its nearest neighbor is approximately equal. Also, each bivalent begins and terminates on the nuclear envelope. These characteristics facilitate reconstruction of the karyotype. In this series of micrographs, the pachytene spindle pole body (Spb) is illustrated in Figures 10–12 and the nucleolus (Nu) in Figures 16–23. In each section, individual synaptonemal complex fragments are numbered according to the bivalent they represent and correspond numerically to those in Table 1 for nucleus A. Some bivalents span only a few sections

TABLE 1. Individual bivalents ranked by relative length for *Melampsora lini*

	Relative length (%/μm)[a]				
	Race 210			Race 01	
Rank	A[b]	B	C	D	E
1	3.2 (4.39)	3.8 (5.06)	3.7 (5.53)	3.5 (4.72)	3.4 (4.69)
2	3.9 (5.45)	3.9 (5.21)	4.0 (5.89)	3.9 (5.24)	3.7 (5.11)*
3	4.0 (5.49)	4.1 (5.42)	4.1 (6.37)*[c]	4.0 (5.41)	4.2 (5.80)
4	4.2 (5.80)	4.2 (5.54)	4.2 (6.38)	4.1 (5.54)*	4.2 (5.87)
5	4.4 (6.06)	4.2 (5.61)	4.6 (6.68)	4.4 (5.90)	4.3 (5.94)
6	4.5 (6.21)*	4.8 (6.35)	4.7 (6.74)	4.5 (6.01)	4.5 (6.21)
7	4.8 (6.59)	4.8 (6.42)*	4.9 (7.32)	4.6 (6.15)	4.8 (6.63)
8	4.9 (6.83)	5.4 (7.08)	5.2 (7.38)	5.1 (6.84)	5.2 (7.18)
9	5.0 (6.90)	5.4 (7.09)	5.2 (7.43)	5.2 (6.93)	5.2 (7.23)
10	5.3 (7.28)	5.4 (7.12)	5.3 (7.92)	5.3 (7.03)	5.5 (7.60)
11	5.4 (7.44)	5.4 (7.12)	5.4 (8.36)	5.4 (7.25)	5.6 (7.73)
12	5.9 (8.15)	5.9 (7.78)	5.8 (8.59)	5.8 (7.78)	5.7 (7.87)
13	6.1 (8.44)	6.0 (7.99)	6.1 (8.81)	5.9 (7.83)	5.8 (8.01)
14	6.6 (9.13)	6.2 (8.20)	6.5 (9.31)	6.3 (8.44)	6.5 (8.98)
15	6.6 (9.13)	6.6 (8.69)	6.5 (9.84)	6.4 (8.60)	6.5 (9.01)
16	7.9 (10.83)	6.9 (9.12)	6.8 (10.04)	7.2 (9.67)	7.0 (9.67)
17	8.1 (11.12)	7.9 (10.46)	8.2 (10.46)	8.5 (11.44)	8.4 (11.60)
18	8.3 (11.40)	8.3 (10.99)	8.3 (11.92)	9.0 (12.02)	8.6 (11.86)

[a] Relative length is the percentage of the total calculated cytological length of the genome. Values in parentheses are in micrometers and are averages of the two lateral elements.

[b] Letters indicate nucleus. Total lengths and volumes are as follows: A, 136.6 μm and 221.0 μm^3; B, 131.2 μm and 179.5 μm^3; C, 142.2 μm and 147.8 μm^3; D, 132.8 μm and 183.2 μm^3; E, 138.1 μm and 192.7 μm^3.

[c] * Indicates NOR-associated bivalent.

(bivalents 1 and 9 in Figs. 33–38 and 17–21, respectively) and most span a moderate number of sections (bivalent 2 in Figs. 19–28), whereas others traverse almost the entire nucleus (bivalent 12 in Figs. 14–33). Generally, longer bivalents tended to span more sections than shorter bivalents, although this was not always the case.

In *M. lini*, the tripartite synaptonemal complex was not as clearly defined as in other heterobasidiomycetes analyzed by the pachytene reconstruction method (4,6,7). With these other fungi, the central element of the synaptonemal complex was used as representative of total bivalent length. In *M. lini*, the central element was often discontinuous from section to section (Figs. 9–38), which precluded its use in measuring bivalent length. The discontinuities may have been due to the incorporation of high concentrations of detergent in the primary fixative (Materials and Methods). Bivalent lengths, therefore, were calculated by averaging the length of the two lateral elements. No clearly defined centromeric regions were resolved at the ultrastructural level for *M. lini*, which precluded the use of the centromeric index for facilitating cross-correlation of bivalents among replicates. Width of the lateral elements was more or less constant along the length of a given bivalent (Figs. 9–38).

Bivalent number and length. Each of the five reconstructed pachytene nuclei in *M. lini* contained 18 distinct bivalents, representing 36 synapsed homologous chromosomes (Table 1). The 18 bivalents ranged from 4.39 to 12.02 μm in length. Relative length (i.e., percentage of the total cytological length) for each bivalent was 3.2–9.0% (Table 1). Bivalents are numbered in order of increasing length in Table 1. Total length of all bivalents was similar among the five reconstructed nuclei, ranging from 131.2

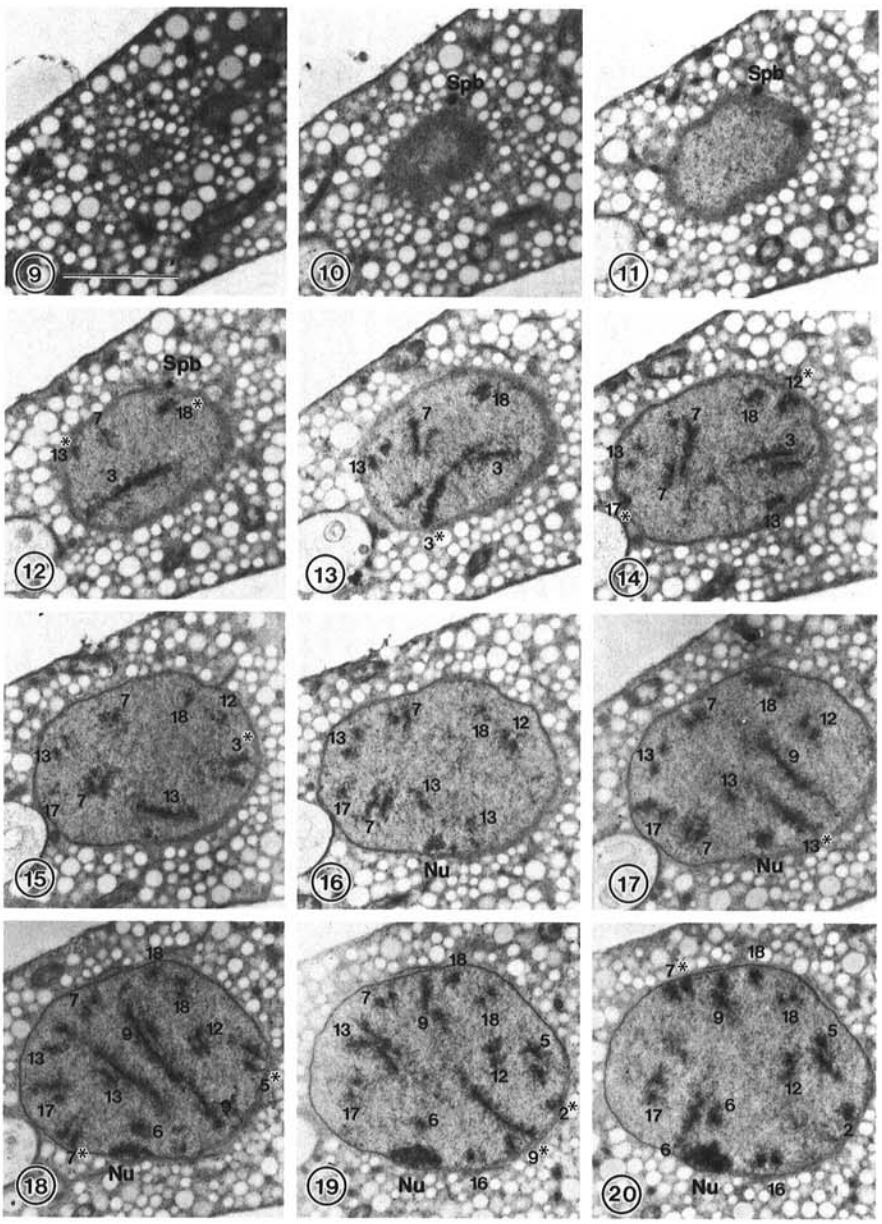

Figs. 9–40. An entire pachytene nucleus of *Melampsora lini* (nucleus A in Table 1) serially sectioned to display the continuity of synaptonemal complex profiles from section to section. This series of electron micrographs illustrates the process by which fragments of the tripartite synaptonemal complex, in consecutive sections, may be followed to determine the individuality of each bivalent. Each bivalent is more or less equidistant from the others, and each begins and terminates on the nuclear envelope (each anchoring site is marked with an asterisk). The NOR bivalent (6 in 18–27) is terminally associated with the nucleolus in Figures 18–22. The pachytene spindle pole body (Spb) is illustrated in 10–12 and the nucleolus (Nu) in 16–23. In each section, individual synaptonemal complex fragments are numbered according to the bivalent they represent and correspond numerically with those presented for nucleus A in Table 1. Bar (Fig. 12) = 3.5 μm. **39** and **40,** A full reconstruction of the nucleus in 9–38 (nucleus A in Table 1), presented from the front (39) and from the rear (40). All bivalents correspond numerically with those in 9–38 and Table 1. Bar (Fig. 39) = 3.5 μm.

to 142.2 μm, as were nuclear volumes (Table 1). However, individual bivalents may not be ranked in exactly the same order among the five nuclei because of similarity in length among adjacent ranks. Additionally, absence of morphological markers other than the association with the nucleolus prevented classification of distinct groups of bivalents.

NOR bivalent. The only bivalent that could be morphologically identified among the five reconstructed nuclei was that associated with the nucleolus (bivalent 6 for nucleus A in Figs. 9–38; Table 1). This bivalent is designated as the NOR bivalent (Table 1). In *M. lini*, the NOR bivalent was terminally associated with the nucleolus in all five nuclei analyzed. An example of this association is presented for nucleus A (Figs. 18–22). Despite some heterogeneity in length for this bivalent among replicate nuclei, the NOR bivalent appeared to be among the shorter chromosomes; the relative length was 3.7–4.8% (Table 1).

DISCUSSION

***M. lini* karyotype.** Ultrastructural analysis of five reconstructed pachytene nuclei provided a definitive karyotype of $n = 18$ for two closely related North American isolates of *M. lini*. The ultrastructural karyotype presented here corrects an earlier estimate from light microscopy of nonpachytene nuclei, which indicated $n = 5$–6 (30). This is not unusual. For many fungi, chromosome counts from light microscopy have underestimated true chromosome numbers when re-analyzed at the ultrastructural level with nuclei in pachynema (4,7–9,12,26,29,35,52). Accordingly, many fungal karyotypes derived from nonpachytene nuclei at the light microscopic level (25,30,46,47) should be treated with caution. Similarly, fungal karyotypes derived by ultrastructural reconstructions of metaphase-anaphase spindles (1,28,38) should be treated with caution because chromosomes at this stage, unlike pachytene bivalents, do not exist as morphologically distinct structures, often are dispersed and move in an asynchronous manner along the length of the spindle, and usually possess minute kinetochoric regions with few attached microtubules (27). Indeed, serial sections through meiotic spindles in metaphase of *Eocronartium muscicola* (5; E. Boehm, *unpublished data*) suggested far fewer chromosomes were present than did reconstructions of pachytene nuclei in this same organism, which established a karyotype of $n = 17$ (6).

The high number of chromosomes reported here for *M. lini* agrees with the high proportion of virulence genes in this pathogen that are reported to segregate independently (18,19,32,33, 51,53). Of the 27 identified virulence genes in *M. lini*, 15 are

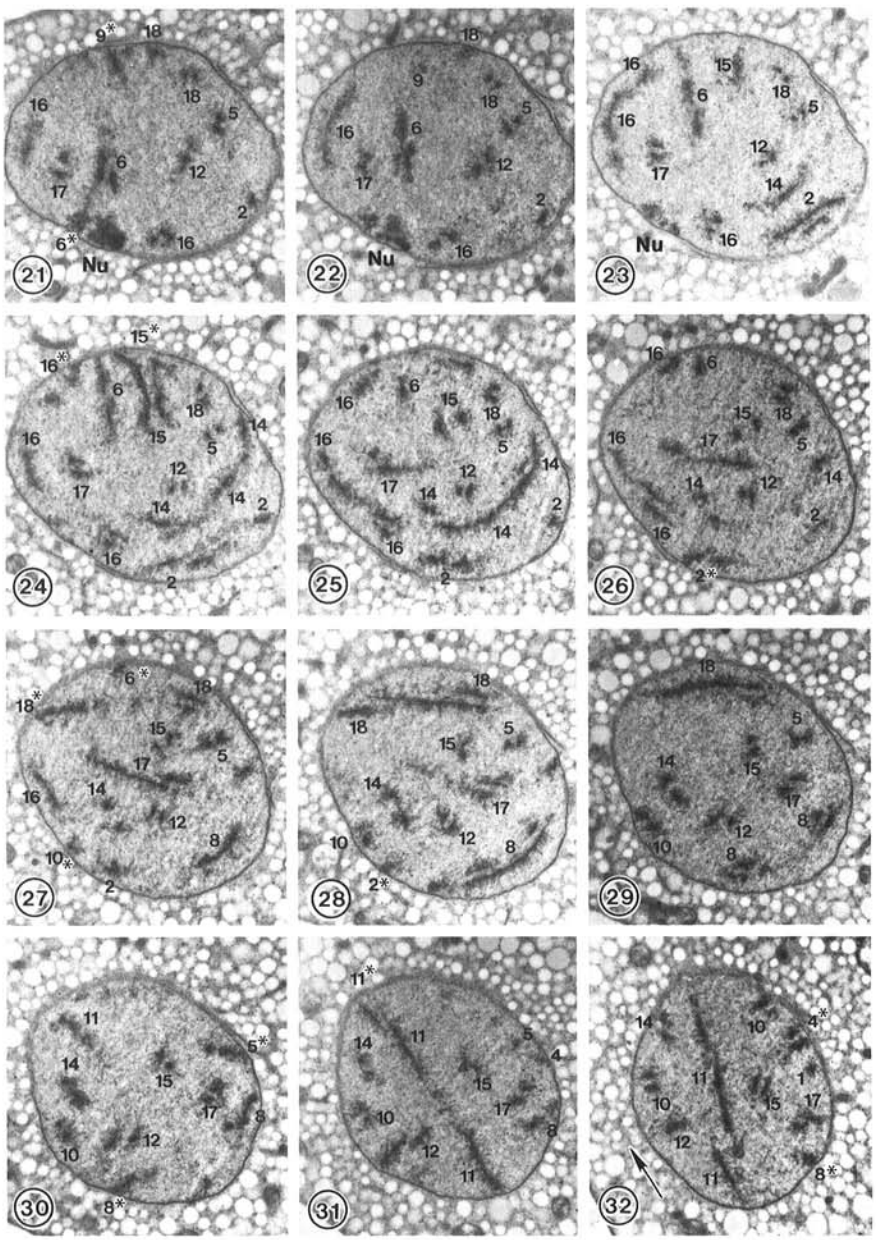

Figs. 21–32. See legend for Figures 9–20.

unlinked and 12 occur in four small groups of four, three, three, and two virulence genes, thus bringing the number of "effective" virulence loci to 19 (32). The ultrastructural pachytene karyotype presented here is in agreement with the genetic data.

The 18 bivalents in *M. lini* formed a finely graded series of chromosome pairs ranging in relative length from 3.2 to 9.0% of the total length. This karyotype is similar to that found for *P. g. tritici*, in which $n = 18$ (7), and *P. coronata*, in which $n = 17$ (4). However, total bivalent length differed among these fungi as follows: *P. coronata*, 75.8 μm (4); *P. g. tritici*, 102.4 μm (7); and *M. lini* (this study) 136.2 μm. If synaptonemal complex length is proportional to genome size (2), data suggest that *M. lini* is 1.3× larger than *P. g. tritici*, which has a relatively large genome, estimated from reassociation kinetics to be 58 Mbp (3). Furthermore, estimates of relative genome size by microscope photometric measurements of fluorescence of propidium-iodide-stained nuclei (14) indicated that the genome is 2.5× larger in *M. lini* than in *P. g. tritici*; the genome of *P. coronata* was 1.1× larger than that of *P. g. tritici*. Despite the discrepancies between estimates based on synaptonemal complex length and nuclear fluorescence, both methods indicate that the genome of *M. lini* is larger than that of *P. g. tritici*, whereas the genome of *P. coronata* is either smaller or only slightly larger than that of *P. g. tritici*.

NOR bivalent. In each reconstructed pachytene nucleus of *M. lini*, a particular bivalent of short relative length was associated with the nucleolus. In other fungi, bivalents cytologically associated with the nucleolus have been shown to carry ribosomal repeats (41). In the absence of the centromeric index (6,12,29), the NOR bivalent was the only one capable of being identified as the same among the five reconstructed nuclei. Unlike *P. g. tritici*, in which the NOR bivalent entered and exited the nucleolus but could not be followed within it (7), in *M. lini* the NOR bivalent was terminally associated with the nucleolus as in *Neurospora crassa* (21), *Schizophyllum commune* (12), *Coprinus cinereus* (29), and *Sordaria macrospora* (55). Furthermore, in *M. lini*, the NOR bivalent did not exhibit significant length variation among the isolates examined. This contrasts with *P. g. tritici*, in which the NOR bivalent differed in relative length among the six isolates examined (7). This variation suggested that other bivalents in the karyotype of *P. g. tritici* may also exhibit length polymorphisms, whereas for the two isolates of *M. lini* examined in this study, the karyotype appears stable.

Among the four heterobasidiomycetous fungi for which ultrastructural pachytene karyotypes are available (4,6,7; this study), no variation in chromosome number has been found among isolates for a given species. Chromosome length polymorphism has, however, been detected for the NOR bivalent of *P. g. tritici* (7). This contrasts with results using electrophoretic methods for separating fungal chromosomes, in which chromosomes within a species frequently vary in number and length (31,36,49).

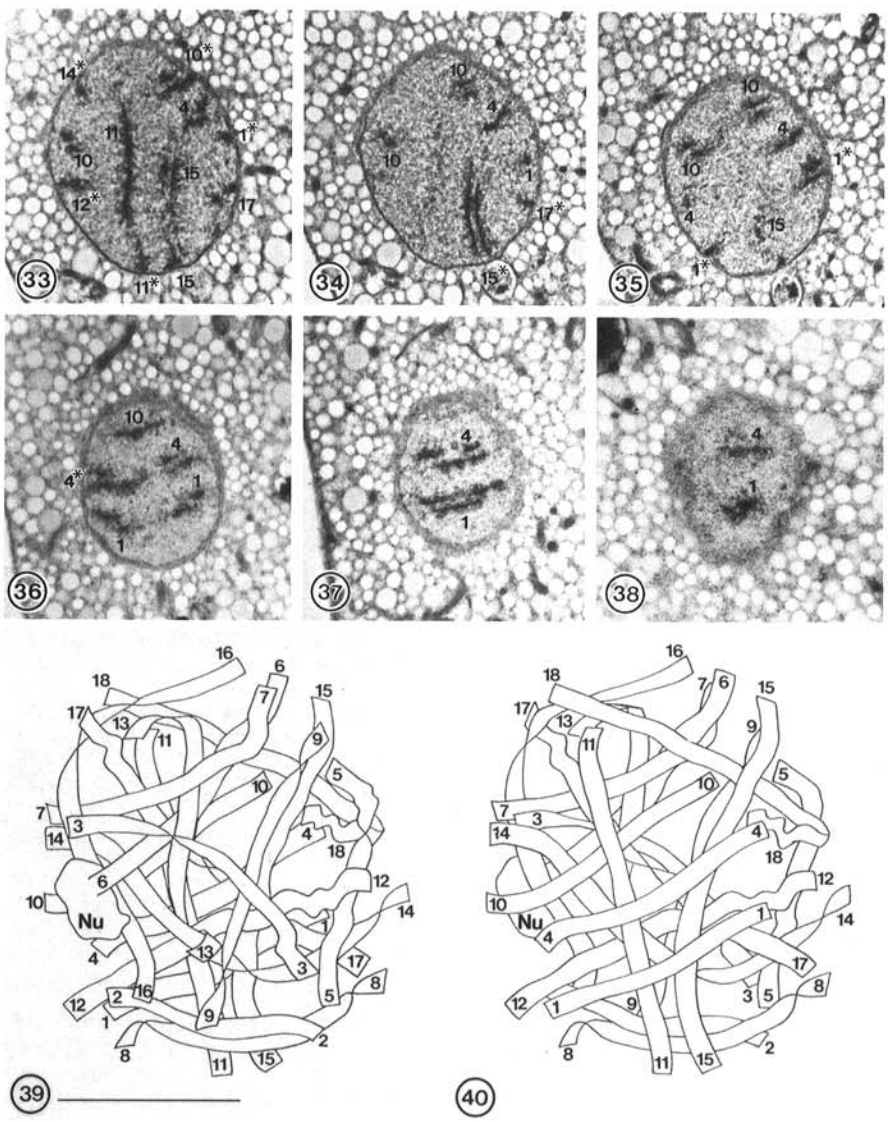

Figs. 33–40. See legend for Figures 9–20.

LITERATURE CITED

1. Aist, J. R., and Bayles, C. J. 1991. Ultrastructural basis of mitosis in the fungus *Nectria haematococca* (sexual stage of *Fusarium solani*) II. Spindles. Protoplasma 161:123-236.
2. Anderson, L. K., Stack, S. M., Fox, M. H., and Chuanshan, Z. 1985. The relationship between genome size and synaptonemal complex length in higher plants. Exp. Cell Res. 156:367-378.
3. Backlund, J. E. 1991. Physical characteristics of the *Puccinia graminis* f. sp. *tritici* genome. M.S. thesis. University of Minnesota, St. Paul. 60 pp.
4. Boehm, E. W. A. 1992. Determination of the karyotype in selected species of *Eocronartium*, *Puccinia* and *Melampsora*. Ph.D. thesis. University of Minnesota, St. Paul. 178 pp.
5. Boehm, E. W. A., and McLaughlin, D. J. 1989. Phylogeny and ultrastructure in *Eocronartium muscicola*: Meiosis and basidial development. Mycologia 81:98-114.
6. Boehm, E. W. A., and McLaughlin, D. J. 1991. An ultrastructural karyotype for the fungus *Eocronartium muscicola* using epifluorescence preselection of pachytene nuclei. Can. J. Bot. 69:1309-1320.
7. Boehm, E. W. A., Wenstrom, J. C., McLaughlin, D. J., Szabo, L. J., Roelfs, A. P., and Bushnell, W. R. 1992. An ultrastructural pachytene karyotype for *Puccinia graminis* f. sp. *tritici*. Can. J. Bot. 70:401-413.
8. Borkhardt, B., and Olson, L. W. 1979. Meiotic prophase in diploid and tetraploid strains of *Allomyces macrogynus*. Protoplasma 100:323-343.
9. Braselton, J. P. 1984. Karyotypic analysis of *Polymyxa graminis* (Plasmodiophoromycetes) based on serial sections of synaptonemal complexes. Can. J. Bot. 62:2414-2416.
10. Braselton, J. P. 1987. Synaptonemal complexes, serial sections and karyotyping. Pages 158-159 in: Zoosporic Fungi in Teaching and Research. M. S. Fuller and A. Jaworski, eds. Southeastern Publishing Corp., Athens, GA.
11. Byers, B., and Goetsch, L. 1975. Electron microscopic observations on the meiotic karyotype of diploid and tetraploid *Saccharomyces cerevisiae*. Proc. Natl. Acad. Sci. USA 72:5056-5060.
12. Carmi, P., Holm, P. B., Koltin, Y., Rasmussen, S. W., Sage, J., and Zickler, D. 1978. The pachytene karyotype of *Schizophyllum commune* analyzed by three dimensional reconstruction of synaptonemal complexes. Carlsberg Res. Commun. 43:117-132.
13. Dresser, M. E., and Giroux, C. N. 1988. Meiotic chromosome behavior in spread preparations of yeast. J. Cell Biol. 106:567-573.
14. Eilam, T., Bushnell, W. R., Anikster, Y., and McLaughlin, D. J. 1992. Nuclear DNA content of basidiospores of selected rust fungi as estimated from fluorescence of propidium iodide-stained nuclei. Phytopathology 82:705-712.
15. Flor, H. H. 1942. Inheritance of pathogenicity in *Melampsora lini*. Phytopathology 32:653-669.
16. Flor, H. H. 1946. Genetics of pathogenicity in *Melampsora lini*. J. Agric. Res. 73:337-357.
17. Flor, H. H. 1954. Identification of races of flax rust by lines with single rust conditioning genes. U.S. Dept. Agric. Tech. Bull. 1087:1-25.
18. Flor, H. H. 1955. Host-parasite interaction in flax rust: Its genetics and other implications. Phytopathology 45:680-685.
19. Flor, H. H. 1956. The complementary genic systems in flax and flax rust. Adv. Genet. 8:29-54.
20. Flor, H. H. 1971. Current status of the gene-for-gene concept. Annu. Rev. Phytopathol. 9:275-296.
21. Gillies, C. B. 1972. Reconstruction of the *Neurospora crassa* pachytene karyotype from serial sections of synaptonemal complexes. Chromosoma 36:119-130.
22. Goetsch, L., and Byers, B. 1982. Meiotic cytology of *Saccharomyces cerevisiae* in protoplast lysates. Mol. Gen. Genet. 187:54-60.
23. Gold, R. E., and Statler, G. D. 1983. Telium formation and teliospore germination in *Melampsora lini*. Can. J. Bot. 61:308-318.
24. Guzman, D., Garber, R. C., and Yoder, O. C. 1982. Cytology of meiosis I and chromosome number of *Cochliobolus heterostrophus* (Ascomycetes). Can. J. Bot. 60:1138-1141.
25. Hansen, E. M., Brasier, C. M., Shaw, D. S., and Hamm, P. B. 1986. The taxonomic structure of *Phytophthora megasperma*: Evidence for emerging biological species groups. Trans. Br. Mycol. Soc. 87:557-573.
26. Harris, S. E., Braselton, J. P., and Miller, C. E. 1980. Chromosomal number of *Sorosphaera veronicae* (Plasmodiophoromycetes) based on ultrastructural analysis of synaptonemal complexes. Mycologia 72:916-925.
27. Heath, I. B. 1978. Experimental studies of mitosis in the fungi. Pages 89-176 in: Nuclear Division in the Fungi. I. B. Heath, ed. Academic Press, New York.
28. Heath, I. B., and Heath, M. C. 1976. Ultrastructure of mitosis in the cowpea rust fungus *Uromyces phaseoli* var. *vignae*. J. Cell Biol. 70:592-607.
29. Holm, P. B., Rasmussen, S. W., Zickler, D., Lu, B. C., and Sage, J. 1981. Chromosome pairing, recombination nodules and chiasma formation in the basidiomycete *Coprinus cinereus*. Carlsberg Res. Commun. 46:305-346.
30. Kapooria, R. G. 1973. Cytological studies of basidiospores of *Melampsora lini*. J. Gen. Microbiol. 75:241-244.
31. Kistler, H. C., and Miao, V. P. W. 1992. New modes of genetic change in filamentous fungi. Annu. Rev. Phytopathol. 30:131-152.
32. Lawrence, G. J. 1988. *Melampsora lini*, rust of flax and linseed. Pages 313-330 in: Advances in Plant Pathology. Vol. 6. Genetics of Pathogenic Fungi. G. S. Sidhu, ed. Academic Press, Orlando, FL.
33. Lawrence, G. J., Mayo, G. M. E., and Shepherd, K. W. 1981. Interactions between genes controlling pathogenicity in the flax rust fungus. Phytopathology 71:12-19.
34. Leung, H., and Williams, P. H. 1987. Nuclear division and chromosome behavior during meiosis and ascosporogenesis in *Pyricularia oryzae*. Can. J. Bot. 65:112-123.
35. Maniotis, J. 1980. Polyploidy in fungi. Pages 163-192 in: Polyploidy: Biological Relevance. W. H. Lewis, ed. Plenum Press, New York.
36. Mills, D., and McCluskey, K. 1990. Electrophoretic karyotypes of fungi: The new cytology. Mol. Plant-Microbe Interact. 3:351-357.
37. Mims, C. W. 1977. Ultrastructure of teliospore formation in the cedar-apple rust fungus *Gymnosporangium juniperi-virginianae*. Can. J. Bot. 55:2319-2329.
38. O'Donnell, K. L., and McLaughlin, D. J. 1981. Ultrastructure of meiosis in the hollyhock rust fungus, *Puccinia malvacearum* II. Metaphase I-telophase I. Protoplasma 108:245-263.
39. Olson, L. W., and Eden, U. M. 1977. A glass bead treatment facilitating the fixation and infiltration of yeast and other refractory cells for electron microscopy. Protoplasma 91:417-420.
40. Person, C. 1959. Gene-for-gene relationships in host-parasite systems. Can. J. Bot. 37:1101-1130.
41. Petes, T. D. 1979. Meiotic mapping of yeast ribosomal deoxyribonucleic acid on chromosome XII. J. Bacteriol. 138:185-192.
42. Pukkila, P. J., and Lu, B. C. 1985. Silver staining of meiotic chromosomes in the fungus, *Coprinus cinereus*. Chromosoma 91:108-112.
43. Raju, N. B. 1986. A simple fluorescent staining method for meiotic chromosomes of *Neurospora*. Mycologia 78:901-906.
44. Sansome, E. R. 1959. Pachytene in *Puccinia kraussiana* Cooke, on *Smilax kraussiana*. Nature (London) 184:1820-1821.
45. Sansome, E. R. 1987. Fungal chromosomes as observed with the light microscope. Pages 97-113 in: Evolutionary Biology of the Fungi. A. D. M. Rayner, C. M. Brasier, and D. Moore, eds. Cambridge University Press.
46. Sherriff, C., and Lucas, J. A. 1989. Cytogenetic study of heterothallic and homothallic isolates of *Peronospora parasitica*. Mycol. Res. 92:302-310.
47. Shirane, N., Masuko, M., and Hayashi, Y. 1989. Light microscopic observation of nuclei and mitotic chromosomes of *Botrytis* species. Phytopathology 79:728-730.
48. Singleton, J. R. 1953. Chromosome morphology and the chromosome cycle in the ascus of *Neurospora crassa*. Am. J. Bot. 40:124-144.
49. Skinner, D. Z., Budde, A. D., and Leong, S. A. 1991. Molecular karyotype analysis of fungi. Pages 86-103 in: More Gene Manipulations in Fungi. J. W. Bennett and L. L. Lasure, eds. Academic Press, San Diego.
50. Slezec, A. M. 1984. Variabilite du nombre chromosomique chez les pleurotes des ombelliferes. Can. J. Bot. 62:2610-2617.
51. Statler, G. D., and Zimmer, D. E. 1976. Inheritance of virulence of race 370, *Melampsora lini*. Can. J. Bot. 54:73-75.
52. Tanaka, K., Heath, I. B., and Moens, P. B. 1982. Karyotype, synaptonemal complexes and possible recombination nodules of the oomycete fungus *Saprolegnia*. Can. J. Genet. Cytol. 24:385-396.
53. Timmis, J. N., Whisson, D. L., Binns, A. M., Mayo, M. J., and Mayo, G. M. E. 1990. Deletion mutation as a means of isolating avirulence genes in flax rust. Theor. Appl. Genet. 79:411-416.
54. von Wettstein, D., Rasmussen, S. W., and Holm, P. B. 1984. The synaptonemal complex in genetic segregation. Annu. Rev. Genet. 18:331-413.
55. Zickler, D. 1977. Development of the synaptonemal complex and the "recombination nodules" during meiotic prophase in the seven bivalents of the fungus *Sordaria macrospora* Auersw. Chromosoma 61:289-316.